Effect of DNA Supercoiling on the Geometry of Holliday Junctions†

Andrey L. Mikheikin, Alexander Y. Lushnikov, and Yuri L. Lyubchenko*

Department of Pharmaceutical Sciences, University of Nebraska Medical Center, Omaha, Nebraska 68198

Received May 19, 2006; Revised Manuscript Received August 8, 2006

ABSTRACT: Unusual DNA conformations including cruciforms play an important role in gene regulation and various DNA transactions. Cruciforms are also the models for Holliday junctions, the transient DNA conformations critically involved in DNA homologous and site-specific recombination, repair, and replication. Although the conformations of immobile Holliday junctions in linear DNA molecules have been analyzed with the use of various techniques, the role of DNA supercoiling has not been studied systematically. We utilized atomic force microscopy (AFM) to visualize cruciform geometry in plasmid DNA with different superhelical densities at various ionic conditions. Both folded and unfolded conformations of the cruciform were identified, and the data showed that DNA supercoiling shifts the equilibrium between folded and unfolded conformations of the cruciform toward the folded one. In topoisomers with low superhelical density, the population of the folded conformation is 50−80%, depending upon the ionic strength of the buffer and a type of cation added, whereas in the sample with high superhelical density, this population is as high as 98−100%. The time-lapse studies in aqueous solutions allowed us to observe the conformational transition of the cruciform directly. The time-dependent dynamics of the cruciform correlates with the structural changes revealed by the ensemble-averaged analysis of dry samples. Altogether, the data obtained show directly that DNA supercoiling is the major factor determining the Holliday junction conformation.

DNA cruciforms play an important role in the regulation of biological processes involving DNA. These structures are formed by inverted repeats and require DNA supercoiling for their stable existence (*1*). Inverted repeats are associated with the origin of replication (*1*−*3*). Cruciforms are suggested to be involved in the regulation of gene expression (*1*, *4*) and may also play a role in nucleosome structure and function (*5*). In addition, the cruciform is an inherent model for the Holliday junction, an intermediate in homologous and site-specific recombination (reviewed in ref *6*). Holliday junctions are also targets for many architectural and regulatory proteins such as histones H1 and H5, topoisomerase IIβ, HMG proteins, HU, p53, and proto-oncogene protein DEK, to mention a few (*7*−*15*). The biological role for some of these interactions is still unclear. Thus far, immobile Holliday junctions or four-way DNA junctions were primary experimental models for structural studies of Holliday junctions by the use of a variety of methods [electrophoresis, fluorescent resonance energy transfer (FRET),[1] X-ray, thermodynamics, and chemical and enzymatic probing (reviewed in refs *6*, *14*, and *16*)]. According to these studies, it can be summarized that the Holiday junction adopts two distinct conformations: folded and unfolded. An unfolded conformation, in which adjacent arms are nearly perpendicular to each other and the structure, has a 4-fold symmetry and exists at a low concentration of metal ions. A folded conformation (or stacked, X-type), in which four arms undergo pairwise coaxial stacking, could be modeled with two duplexes exchanging strands at the junction point. This conformation is stabilized by high ionic strength di- or polyvalent cations in particular (e.g., Mg^{2+} cations at a concentration of more than 100 μM). Sodium cations also shift equilibrium distribution toward a folded conformation, although much higher concentrations of cations are required (*17*). Also, a folded conformation of cruciform can be parallel or antiparallel. The synthetic immobile DNA junction exists in antiparallel geometry, and no parallel geometry was observed (*6*, *16*, *18*, *19*). However, computer modeling showed that the interarm angle can vary in a broad range of values (*20*). Furthermore, thermodynamic studies on short Holliday junctions tethered to form parallel or antiparallel orientation revealed that there is no significant difference in free energy between these orientations (*21*).

Atomic force microscopy (AFM) was successfully applied for imaging cruciforms in supercoiled DNA (*5*, *22*−*24*). These early studies showed that the cruciform in supercoiled DNA can adopt folded and unfolded conformations, but in a folded conformation, a parallel rather than an antiparallel orientation of the helical strands is observed. It was hypothesized that DNA supercoiling is an important factor in such a conformational preference for the cruciform (*5*, *24*). To test this hypothesis, we systematically analyze the structural and dynamic properties of the cruciform in plasmids with different superhelical densities. We employed

† This research was supported by Grant GM 062235 (to Y.L.L.) from the National Institutes of Health.

* To whom correspondence should be addressed: Department of Pharmaceutical Sciences, College of Pharmacy, University of Nebraska Medical Center, 986025 Nebraska Medical Center, Omaha, NE 68198-6025. Telephone: 1-(402)-559-1971. Fax: 1-(402)-559-9543. E-mail: ylyubchenko@unmc.edu.

[1] Abbreviations: AFM, atomic force microscopy; APS, 1-(3-aminopropyl)silatrane; FRET, fluorescent resonance energy transfer.

10.1021/bi061002k CCC: $33.50
Published on Web 10/07/2006

AFM, including the time-lapse imaging in aqueous solutions, to study the cruciform structure in buffers with different concentrations of metal ions. The results presented here indicate that the geometry of cruciform is primarily governed by DNA supercoiling. DNA supercoiling shifts equilibrium between folded and unfolded conformations of cruciform toward the folded one with the parallel orientation of the DNA helical strands rather than the antiparallel configuration typically observed in synthetic Holliday junctions. The effect of DNA supercoiling is enhanced in the presence of cations. These findings provide additional support for studies on the role of DNA supercoiling in the structure and dynamics of Holliday junctions (cruciforms).

MATERIALS AND METHODS

Plasmids. Topoisomer samples of plasmid pFR6 (3396 bp) (a kind gift from V. Potaman, Texas A&M University) are prepared as described earlier (*22*, *25*). Each topoisomer sample contains a set of topoisomers and is characterized by the mean value of superhelical density $\langle\sigma\rangle$. Two topoisomer samples, one with low superhelical density denoted as $t3_{low}$ (mean value $\langle\sigma\rangle = -0.038$) and another with high superhelical density denoted as $t7_{high}$ (mean value $\langle\sigma\rangle = -0.085$), are used for analysis of cruciform geometry and dynamics.

Synthetic DNA Holliday Junction. The synthetic DNA Holliday junction with two arms of 320 bp and two arms of 64 bp symmetrically positioned relative to the center of the junction was synthesized by ligation of DNA fragments to the core structure of the immobile Holliday junction. The core structure of the Holliday junction was obtained by stepwise annealing of four oligonucleotides. The detailed procedure can be found in the Supporting Information.

AFM Procedure. The AFM procedure was performed as described earlier (*22*, *23*, *25*−*28*) A mica surface was modified for 30 min with 0.5 mM 1-(3-aminopropyl)silatrane [APS (*26*)] for experiments in solution and with 0.16 mM APS for imaging dried samples. The sample was deposited on APS-modified mica for 2−5 min, then rinsed with deionized water, and dried with argon (for the experiment with a dried sample) or applied directly without a rinsing/drying procedure for AFM imaging with a hydrated sample.

Time-lapse Imaging. Time-lapse imaging in hydrated samples was performed as described earlier (*24*, *27*). Briefly, the APS-modified mica with the sample droplet on the top of it was placed on the scanning stage of MultiMode SPM Nanoscope IIIa (Veeco, Santa Barbara, CA). The optical head with an installed liquid cell was mounted above the sample; additional buffer was added into the space between the cell and mica surface; and the scanning tip (NP probe, Veeco, Santa Barbara, CA) was approached to the surface and engaged. The buffer was replaced when necessary, with two syringes attached to the flow cell, without terminating the scanning.

Samples $t3_{low}$ and $t7_{high}$ were prepared and imaged in the following buffers: HE buffer [10 mM *N*-2-hydroxyethylpiperazine-*N*′-2-ethanesulfonic acid (HEPES) and 1 mM ethylenediaminetetraacetic acid (EDTA) at pH 7.0], HEN buffer (10 mM HEPES, 1 mM EDTA, and 200 mM NaCl at pH 7.0), and HM buffer (10 mM HEPES and 10 mM $MgCl_2$ at pH 7.0).

The short synthetic Holliday junction was prepared and imaged in TE buffer (10 mM TRIS-HCl and 1 mM EDTA at pH 7.0) and TM buffer (10 mM TRIS and 10 mM $MgCl_2$ at pH 7.0).

Data Analysis. Data analysis was performed using the FemtoScan Online software package (version 1.6 (4.4); Moscow State University and Advanced Technologies Center, Moscow, Russia). The angles between DNA helices at junction point were measured as described in our recent paper (*28*). To measure the angle value, lines were drawn over the middle of DNA filaments just near the junction point over the filament sections ca. 10 nm that typically appears as straight lines. The angle between these lines was measured (see Figure S1 in the Supporting Information for specifics). Because the cruciform hairpin arms are not necessary continuations of the plasmid main strands, both the angles between the hairpin arm and the angles between DNA main strands were measured. Lengths of cruciform arms were measured as described before (*27*). A cruciform arm was approximated by a segmented line, and the length of the arm was obtained from the sum of the segment lengths (see Figure S1 in the Supporting Information for specifics).

RESULTS

The Cruciform Structure—Effect of DNA Supercoiling. The schematics of cruciform (Holliday junction) conformations are presented in parts a−e of Figure 1. The DNA helices are shown as cylinders, and the round-shaped caps on them correspond to loops of the hairpin arms of the cruciform. The structure depicted in Figure 1a corresponds to the unfolded (open) conformation of the cruciform, whereas parts b and c and d and e of Figure 1 show two orthogonal views of folded conformations with parallel or antiparallel orientation of helical strands, respectively. Projections c and e are obtained by rotation of projections b and d, respectively, by 90° around the vertical axis.

Figure 1f shows the AFM image of the synthetic Holliday junction assembled from four linear arms in TEM buffer. Folded and unfolded conformations of the junction on the AFM image could be found and are marked with F and U, respectively. Typical images of supercoiled DNA molecules with the cruciform in unfolded and folded conformations are shown in Figure 2a (sample $t3_{low}$, $\langle\sigma\rangle = -0.038$ in HE buffer) and Figure 2b (sample $t7_{high}$, $\langle\sigma\rangle = -0.085$ in HE buffer), respectively. The AFM images for the sample with low supercoiling density ($t3_{low}$) reveal both folded and unfolded conformations of cruciforms, but the cruciform appears in a folded conformation for sample $t7_{high}$ (Figure 2b). To quantify this effect, we counted the occurrence of both conformations of Holliday junctions; we found that folded conformation exists in 16, 48, and 98% of short Holliday junctions and samples $t3_{low}$ and $t7_{high}$, respectively (see Table 1).

Effect of Ionic Conditions on Conformational Transitions of the Cruciform. Ionic conditions have a profound effect on the conformations of immobile Holliday junctions. What is the effect of ionic strength and divalent cations on conformations of Holliday junctions under the negative supercoiling stress? To answer this question, we performed imaging of $t3_{low}$ and $t7_{high}$ samples as well as synthetic Holliday junctions at various ionic conditions. Images presenting folded and unfolded conformations for different

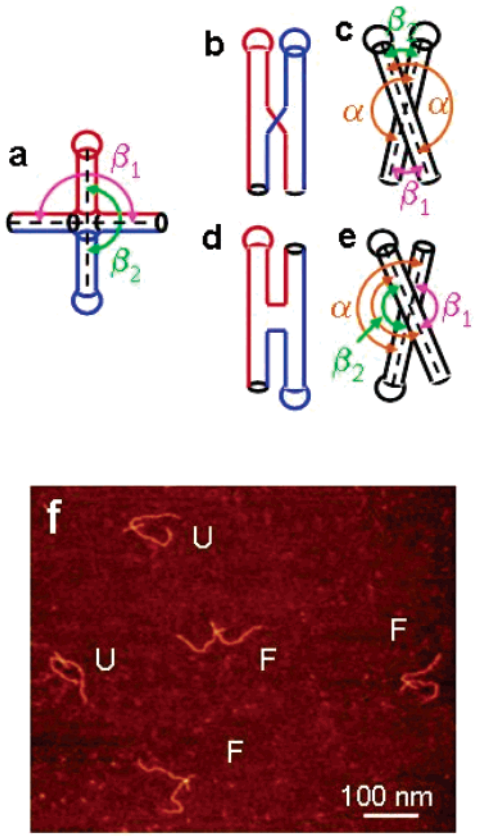

FIGURE 1: Schematic representation of cruciform conformations: unfolded (a) and folded (b−e) conformations with parallel (b and c) and antiparallel (d and e) orientations of DNA strands. Complementary DNA strands are indicated with red and blue colors. Arches with arrows of different colors show "stacking" angle α (brown), the angle between main DNA strands β_1 (pink), and the angle between hairpin arms β_2 (green). (f) AFM image of the dried sample for the synthetic Holliday junction deposited from TM buffer. "F" and "U" denote Holliday junctions in folded and unfolded conformations, respectively.

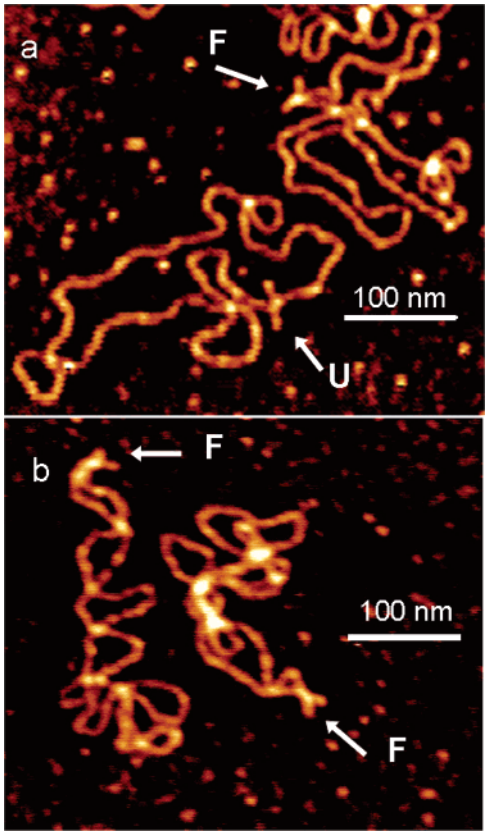

FIGURE 2: AFM images of dried sample $t3_{low}$ (a) and sample $t7_{high}$ (b) deposited from HE buffer. "F" and "U" denote cruciform in folded and unfolded conformations, respectively. The arrow shows the position of cruciform in the DNA molecule.

samples are shown in Figures 1f and 2. First of all, we analyzed the partition of the Holliday junctions between the unfolded and folded conformations as a function of the buffer composition and DNA supercoiling. Results of this analysis are summarized in Table 1. The cruciform in sample $t7_{high}$ predominantly (98%) adopts a folded conformation, even in low ionic strength buffer; therefore, the distribution between two conformations very slightly depends upon the ion concentration. Quite different results were obtained for sample $t3_{low}$ and synthetic Holliday junctions. The population of both conformations for the sample $t3_{low}$ remains nearly equal when buffer with low ionic strength is used, whereas 10 mM Mg^{2+} significantly shifts equilibrium between the folded and unfolded conformations of the cruciform toward the folded one. Synthetic Holliday junctions adopt an unfolded conformation in HE buffer, but the addition of 10 mM Mg^{2+} also shifts equilibrium toward the folded one. These data are in qualitative agreement with corresponding data in solution (*6*, *18*, *19*).

Geometry of the Cruciform in the Folded Conformation. The AFM data allow us to characterize conformations of the cruciforms. According to the schematics for the Holliday junction (parts b−e of Figure 1), angle α between the hairpin arm and its continuation in the main DNA strands when equal to 180° indicates the stacking of these arms. At the same time, angle β_2 between the hairpin arms or angle β_1 between long DNA strands allows us to distinguish between the parallel conformation (schemes b and c in Figure 1, acute angles β_1) and the antiparallel conformation (schemes d and e in Figure 1, obtuse angles β_1). To retrieve this information, we performed angle measurements between all arms of the cruciform.

A set of the large number of images (between 86 and 150 frames) was obtained for each sample in different ionic conditions (HE, HEN, and HM buffer). Figure 3 shows the results for the measurements of the interarm angle α (see parts c and e of Figure 1 for the explanations). The histograms for the distribution of angle α values obtained for sample $t7_{high}$ in HM buffer (Figure 3a) and for sample $t3_{low}$ in HE buffer (Figure 3b) are centered around the 180° value. The distributions are quite narrow, suggesting that the hairpin arm is a continuation of the corresponding main strand, or in other words, the sections of the cruciform are stacked. Similar results were obtained for sample $t3_{low}$ in HEN and HM buffers as well as for sample $t7_{high}$ in HE and HEN buffers (data not shown).

Another set of angles provides the information on the type of the folded conformation, parallel or antiparallel. These are the angles between the hairpin arms and the main strands, β_1 (see parts c and e of Figure 1 and the Materials and Methods for specifics). If the angle is less than 90°, the conformation of the cruciform is referred to as the parallel conformation; if the angle is more than 90°, the helices are in antiparallel orientation (*24*). Two typical histograms of the angle distributions for β_1 angles are shown in parts a

Table 1: Occurrence (Percent) of Folded and Unfolded Conformations in the Synthetic Holliday Junction and in Topoisomer Samples $t3_{low}$ and $t7_{high}$[a]

	HE		HEN		HM	
buffer	folded	unfolded	folded	unfolded	folded	unfolded
synthetic Holliday junction	16[b] (37)	84[b] (195)			48[c] (98)	52[c] (107)
$t3_{low}$	48 (125)	52 (136)	52 (127)	48 (115)	81 (182)	19 (42)
$t7_{high}$	98 (288)	2 (5)	99 (148)	1 (1)	100 (150)	0 (0)

[a] The number of molecules measured for specific conformation is shown in parentheses. [b] In TE buffer. [c] In TM buffer.

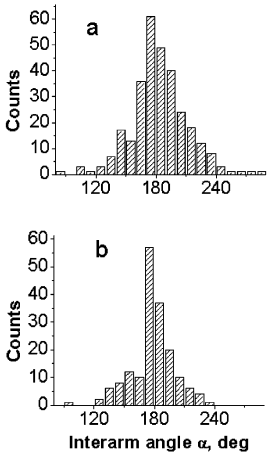

FIGURE 3: "Stacking" angle α (see schematics in parts c and e of Figure 1) measured for dried samples: (a) sample $t7_{high}$ deposited in HM buffer and (b) sample $t3_{low}$ deposited in HE buffer.

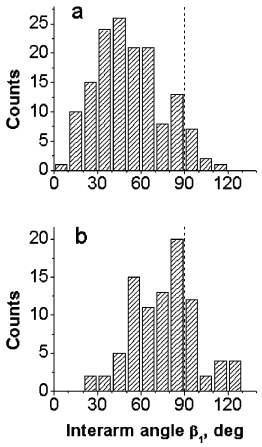

FIGURE 4: Angle β_1 between main DNA strands for cruciform in a folded conformation (see schematics in parts c and e of Figure 1) measured for dried samples: (a) sample $t7_{high}$ deposited from HM buffer and (b) sample $t3_{low}$ deposited from HE buffer.

and b of Figure 4 for sample $t7_{high}$ in HM buffer and for sample $t3_{low}$ in HE buffer, respectively. A dashed vertical line is drawn at 90°. The points to the left of this line correspond to the parallel orientation of the cruciform, whereas all points to the right of these lines correspond to the antiparallel one. Figure 4a shows that the cruciform for the $t7_{high}$ sample adopts a folded conformation with a parallel orientation of the arms. At lower supercoiling density (sample $t3_{low}$, Figure 4b), the preference to the parallel configuration remains, although the entire distribution is shifted to greater angle values. The mean values of β_1 angles and their standard deviations calculated from similar measurements are summarized in Table 2. The data show that cruciforms in the two samples at different ionic conditions adopt parallel orientation, whereas the synthetic Holliday junction at 10

Table 2: Angle β_1 (see Schematics in Parts c and e of Figure 1) Measured for Cruciform in a Folded Conformation for the Synthetic Holliday Junction and for Topoisomer Samples $t3_{low}$ and $t7_{high}$ in Different Buffers[a]

buffer	HE	HEN	HM
synthetic Holliday junction	N/A		95 ± 40 (205)[b]
$t3_{low}$	75 ± 21 (90)	67 ± 23 (92)	68 ± 29 (106)
$t7_{high}$	76 ± 22 (86)	64 ± 23 (148)	52 ± 24 (150)

[a] The number of measured molecules is shown in parentheses. [b] In TM buffer.

mM $MgCl_2$ predominantly adopts an antiparallel orientation. The data on the orientation of DNA arms in synthetic Holliday junctions is in qualitative agreement with corresponding results obtained in solution (*6*, *17*). It is should also be noted that Mg^{2+} folds the cruciform even more tightly, increasing the effect of the supercoiling. Monovalent cations work in the same way, but the effect is considerably less pronounced than that of the divalent cations.

Geometry of the Cruciform in the Unfolded Conformation. The set of data obtained allows us to analyze the geometry of the unfolded conformation of the cruciform, which could be found in the $t3_{low}$ sample at low ionic strength conditions. We measured all four angles between adjacent arms to characterize this conformation. These angles are $85-94 \pm 27°$, suggesting that the unfolded conformation of the cruciform is close to a planar geometry and has 4-fold symmetry. These values correlate well with data obtained by other methods (*29*).

Time-lapse Observations of the Cruciform Conformational Dynamics. To study the dynamics of the cruciform, we performed time-lapse imaging and captured a large series of consecutive images for the same molecules in aqueous solutions without drying the sample (*24*, *27*).

Selected time-lapse images illustrating the dynamics of the cruciform for samples $t3_{low}$ and $t7_{high}$ in HE buffer are presented in Figure 5. The cruciform in sample $t3_{low}$ (parts a−f of Figure 5) shows high conformational dynamics. It changes conformation several times and flips from the folded to the unfolded and back to the folded conformation several times during the course of the experiment. Parts g−k of Figure 5 in which traces of the cruciform only are shown summarizes these conformational changes [these images are made by placing traces of molecules on a black background as described earlier (*27*)]. The full set of data that comprises 91 frames assembled as a movie file can be viewed in the Supporting Information. File S1A was assembled from unprocessed AFM images of the molecule sections containing the cruciform, and file S1B was assembled from the images of the cruciform traces placed on a black background and centered at the junction. Similar data were obtained for

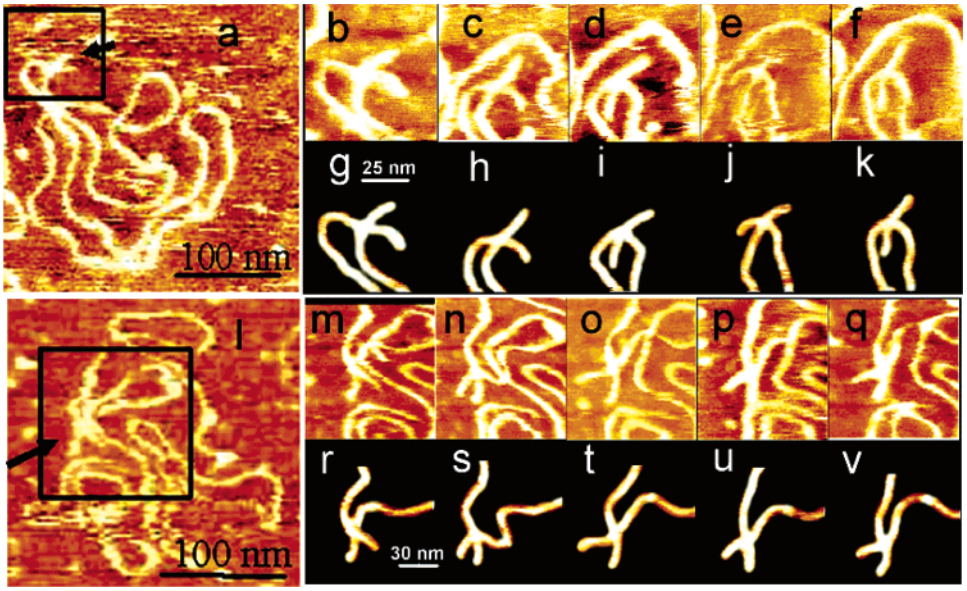

FIGURE 5: Dynamics of the cruciform observed with time-lapse AFM for hydrated sample $t3_{low}$ (frames a−k) and sample $t7_{high}$ (frames l−v) in HE buffer. The initial image of the molecule with cruciform is shown in frame a (sample $t3_{low}$) and frame l (sample $t7_{high}$). The arrow is pointed to the cruciform. Images of an enlarged area specified by the square in the initial image show the time progress of the cruciform structure (frames b−f for sample $t3_{low}$ and frames m−q for sample $t7_{high}$). Traces of the same molecule on a black background are shown in frames g−k (sample $t3_{low}$) and frames r−v (sample $t7_{high}$). The capture time for images are 0 min (a), 11 min (b), 44 min (c), 60 min (d), 134 min (e), and 155 min (f) (for sample $t3_{low}$) and 0 min (l), 13 min (m), 22 min (n), 71 min (o), 233 min (p), and 363 min (q) (for sample $t7_{high}$).

other molecules in separate time-lapse experiments. Interestingly, transitions from folded to unfolded states and vice versa appeared as two-state flips; therefore, we were unable to observe transient states between the two conformations, suggesting that the lifetime of these states is much shorter than the image acquisition time.

The results for the cruciform dynamics within the plasmid with high supercoiling density (sample $t7_{high}$) obtained in one time-lapse experiment are shown in parts l−q of Figure 5. This cruciform remains in a folded conformation even over an observation period of 9.5 h. Other observations with the same $t7_{high}$ sample were consistent with this long one; we were unable to detect the transition between folded and unfolded conformations. The only change was the variation of the angle between the arms. These dynamics are summarized in parts r−v of Figure 5, and the full set of data is placed as movie files in the Supporting Information. File S2A is assembled from unprocessed AFM images of the molecule sections containing the cruciform. File S2B was assembled from the images of the cruciform traces placed on a black background and centered at the junction. Overall, the time-lapse observations showed that the cruciform undergoes conformational transitions if the supercoiling density is low (sample $t3_{low}$) but that the conformation does not change if the supercoiling density is high. This conclusion is consistent with the data obtained in the studies of dried samples when the analysis was performed by averaging over an ensemble of molecules (see Table 1). These data show that the populations of folded and unfolded conformations of the cruciform were nearly equal for the $t3_{low}$ sample, whereas equilibrium distribution between these conformations in the $t7_{high}$ sample is shifted toward the folded one.

To quantify the data on dynamics, we measured the "stacking" of α angles in the folded conformation of the cruciform in the same way as the dried samples (for a definition, see parts c and e of Figure 1). We assembled the

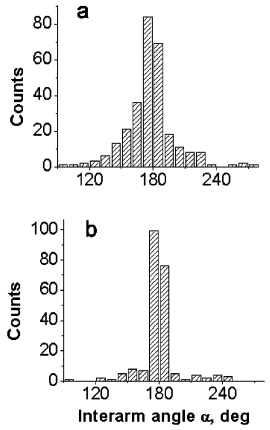

FIGURE 6: "Stacking" angle α (see schematics in parts c and e of Figure 1) measured in hydrated sample: (a) sample $t7_{high}$ in HM buffer and (b) sample $t3_{low}$ in HE buffer.

data from several molecules. Two representative histograms of distributions are presented in Figure 6a (sample $t7_{high}$ in HM buffer) and Figure 6b (sample $t3_{low}$ in HE buffer). Similar results were obtained in the case of sample $t3_{low}$ in HEN and HM buffer as well as for sample $t7_{high}$ in HE and HEN buffer (data not shown). Similar to dried samples, the maxima of these peaks are centered at ∼180° and the widths are quite narrow.

We also plotted the interarm angles (see Figure 1) as a function of time. The graphs for the time-lapse experiments for two molecules of $t3_{low}$ and $t7_{high}$ samples in HE buffer are shown as time trajectories in parts a and b of Figure 7, respectively (the same molecules are presented in Figure 5 and as movie files in the Supporting Information). The data for both angles are indicated in pink and green colors for β_1 and β_2, respectively (the same colors as in parts a, c, and e of Figure 1). Vertical dashed lines in Figure 7a separate regions between different conformations of the cruciform

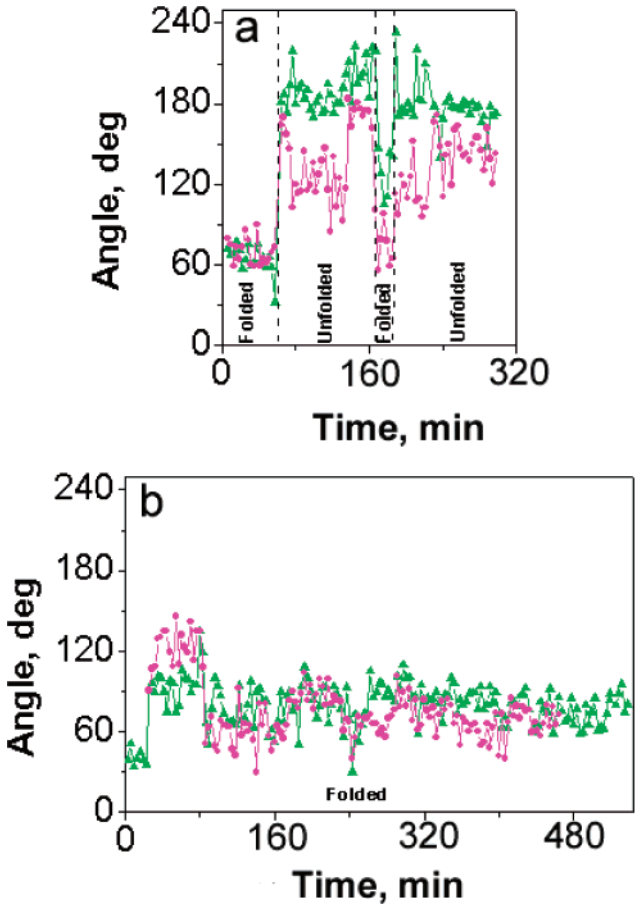

FIGURE 7: Dynamics of the time-dependent variation of angle β_1 (pink line) and angle β_2 (green line) (see schematics in parts a, c, and e of Figure 1) for samples $t3_{low}$ (a) and $t7_{high}$ (b) in HE buffer. The vertical dashed lines indicate the change in cruciform conformation as named on the bottom of the graph. The time difference between two consecutive frames is ~3 min.

(folded or unfolded). The changes of conformation of cruciforms are clearly seen from Figure 7a. The cruciform is initially in a folded conformation, and both β_1 and β_2 are ~70°. Then, the conformation of the cruciform changes to the unfolded conformation, and this transition is accompanied by a significant change in the angle value (from ~70° to ~180°). The cruciform remains in an unfolded conformation for some time, and the β_2 angle fluctuates around 180°, whereas the β_1 angle varies between ~100° and ~180°. Then, conformation changes to the folded conformation, and both of the β_1 and β_2 values drop to ~100°. Finally, the cruciform changes conformation to the unfolded conformation, with both angles becoming closer to 180°. Similar experiments with sample $t7_{high}$ did not reveal any transition between the conformations of the cruciform in sample $t7_{high}$ (see Figure 7b); values for β_1 and β_2 angles vary between ~40° and ~140°, although some dynamics of the cruciform within the family of the folded conformation was observed. For example, the interarm angles β_2 and β_1 are >90° for frames between 8 and 25, corresponding to the antiparallel orientation of cruciform arms (see Figure 1), whereas for the rest of this graph, angle values are <90°; therefore, this orientation is parallel. As also seen from this figure, both β_1 and β_2 angles change in a coordinated manner. Such a correlated mobility confirms the conclusion made earlier that the hairpin arms and the main strands of the cruciforms are stacked. To find the mean value of angle β_1, we assembled

Table 3: Angle β_1 (see Schematics in Parts c and e of Figure 1) Measured for Cruciform in a Folded Conformation for Dried and Hydrated Samples $t3_{low}$ and $t7_{high}$

	HE		HM	
buffer	dry sample	in buffer	dry sample	in buffer
$t3_{low}$	75 ± 21	74 ± 18	68 ± 29	66 ± 24
$t7_{high}$	76 ± 22	70 ± 24	52 ± 24	44 ± 23

data from several molecules, and the total number of images analyzed was not less than 100 in each case. We found that the mean values of angle β_1 of cruciforms in fully hydrated samples are quite similar to corresponding values found for dried samples (see Table 3). The highest difference between the data for dried samples and in solution is 8° (with a standard deviation of 23°) for sample $t7_{high}$ in HM buffer; therefore, it can be concluded that data in dried sample are consistent with the time-lapse data obtained in buffer.

Branch Migration. We measured the lengths of the hairpin arms for the time-lapsed images to evaluate the effect of the supercoiling on branch migration. A similar approach was applied in our paper (*27*) for analysis of branch migration in synthetic Holliday junctions. We plotted time-dependent variation of the lengths of cruciform hairpin arms of the $t3_{low}$ sample in unfolded (Figure 8a) and folded (Figure 8b) conformations in HE buffer, assembling the results for various experiments that are separated by vertical dashed lines. The data for two hairpin arms are indicated with different colors. Some sections of the time trajectories for unfolded cruciforms (Figure 8a, molecules III and IV) show a gradual change in the hairpin lengths in which both hairpins increase (molecule III) and decrease (molecule IV) their length, and these changes exceed the noise-level fluctuations of the arm lengths (these change are marked with arrows). Importantly, both hairpins change their length in a coordinated manner. Such a coordinated change in the hairpin arm length was not observed for folded cruciforms (Figure 8b). This finding is consistent with the model in which unfolding of the Holliday junction is required for branch migration (*19*, *27*, *30*, *31*).

DISCUSSION

The interplay between the local DNA structures and the global DNA conformations (topology) plays a significant role on DNA functions. The cruciforms formed by inverted repeats in supercoiled DNA are alternative DNA structures that are critically involved in various DNA transactions. Cruciforms adopt different conformations. This conformational transition can have a strong effect on the global DNA structure and dynamics, playing the role of a molecular switch, influencing the search of homologous regions within the supercoiled DNA molecule or in a topological domain (*5*). In our early paper (*24*), we applied for the first time AFM for direct imaging of the cruciform dynamics; we were able to characterize the transition between folded and unfolded conformations of the cruciforms. These data suggested that DNA supercoiling can be a critical factor determining the conformation of the cruciform. The results obtained in this paper not only support this hypothesis but also provide a number of important characteristics to the structure and dynamics of the cruciform, depending upon the DNA supercoiling and ionic conditions. Importantly,

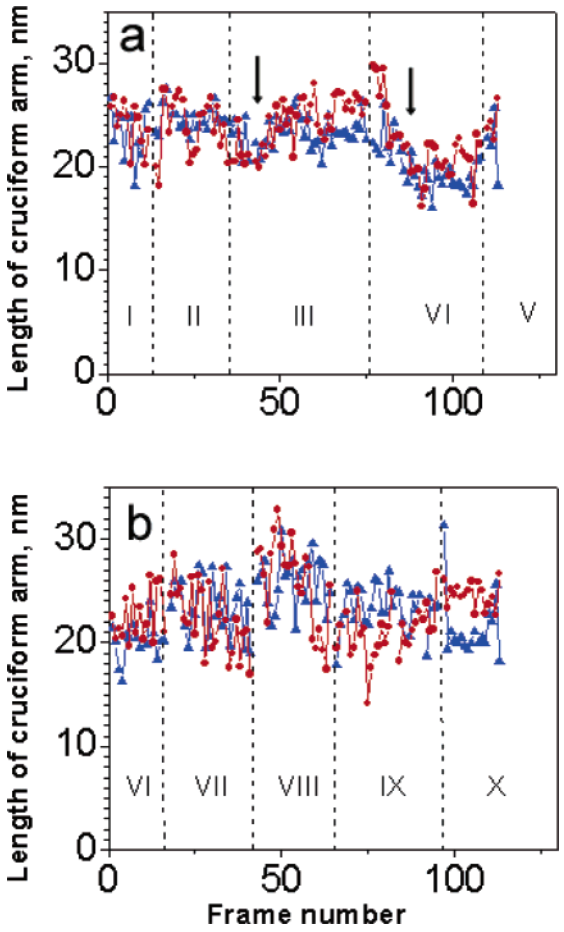

FIGURE 8: Time-dependent variation of the length for hairpin arms measured in selected molecules with cruciform in an unfolded conformation (a, molecules I−V) and in a folded conformation (b, molecules VI−X) for sample $t3_{low}$ in HE buffer. Vertical dashed lines separate data for different molecules. Arrows indicate the area when the arm length starts to change significantly (see the text for details).

these studies revealed some similarities while also revealing drastic differences between the four-way junction with free ends (synthetic Holliday junctions) and the cruciforms, the mobility of which is limited by the DNA topology.

Both synthetic junctions and cruciforms are capable of forming unfolded and folded states, but in contrast to synthetic junctions, the conformation of which is determined by ionic conditions, primarily by the presence of divalent cations, the DNA supercoiling is the most critical factor in determining the cruciform conformation. Therefore, the cruciform in sample $t7_{high}$ (high supercoiling density) adopts predominately the folded conformation even at low ionic strength and the absence of Mg^{2+} cations, although these cations further shift the equilibrium between the folded and unfolded conformations toward the folded conformation. The cruciforms in sample $t7_{high}$ in the presence of Mg^{2+} cations fold tighter, which makes hairpin arms approach each other very closely.

The most dramatic difference between the structural features of cruciforms and synthetic Holliday junctions is the geometry of the folded conformation. It was shown that, in the absence of the topological constraints and in the presence of divalent cations, Holliday junctions fold to the conformation with an antiparallel orientation of the exchanging arms (*6*, *16*, *18*, *19*). Our data show that the cruciform adopts a parallel configuration of exchanging arms even in the absence of divalent cations. The cations further enforce this conformation of the cruciform. These findings suggest that negative DNA supercoiling stabilizes the folded conformation with a parallel orientation of the arms. What is the energetic difference in these two conformations of the junction? Does the DNA supercoiling provide sufficient energy to stabilize an alternative conformation? Thermodynamic analysis of the stability between the parallel and antiparallel conformations performed on tethered junctions (*21*) revealed rather small differences in free energies for these two states (ca. 1.5 kcal/mol) in favor of antiparallel geometry. The molecular-modeling analyses (*20*) came to qualitatively similar conclusions, although the free energy for the antiparallel conformation was estimated at 18 kcal/mol lower than that for the parallel conformation. It is instructive to compare these values with the free energy of DNA supercoiling. According to the well-known expression for the free energy of DNA supercoiling, $\Delta G = 1100RT(\Delta Lk)^2/N$, where R is the gas constant, T is the temperature (in Kelvin), N is the length of the plasmid in base pairs, and ΔLk is the linking number difference that is proportional to the supercoiling density σ value [$\Delta Lk = N/\gamma$, where γ is the number of base pairs per turn in linear DNA (*1*, *32*)]. For the plasmid used in this work ($N = 3396$ bp), the free-energy increment per one supercoiling turn estimated for the supercoiling density close to the transition value [$\Delta Lk = 13$ (*22*)] is ca. $8.4RT$ or 5 kcal/mol. This estimate shows that supercoiling energy is in the range sufficient for stabilizing the unfavorable folded conformation of the junction. The stabilization of unfavorable DNA conformations is a ubiquitous property of negative DNA supercoiling, facilitating dramatically different dynamics of DNA required for its functioning. The fact that unwinding stress is needed for the folding of the junction into a parallel conformation can be useful in modeling folded conformations of the Holliday junctions.

The measurements of the angles between the arms of the cruciforms showed that the hairpin arm and one of the arms of the main DNA strand form an almost continuous helix. Moreover, our time-lapse experiments show that these arms move in a coordinated manner. These findings suggest that the helices interact within the joint point probably because of the stacking between the helices. A similar stacking interaction was observed for the antiparallel conformation of the Holliday junction recently confirmed by X-ray crystallographic analyses (*14*, *16*). Recent single-molecule three-color FRET studies of the synthetic Holliday junction showed a coordinated movement the arms during the junction dynamics between the two folded states (*33*). Altogether, these data show that the interhelical interaction at the joint is a common feature for such branched DNA structures and that the most favorable configuration for the helices arrangement dictates the DNA topology and environmental conditions such as ionic strength. The time-lapse AFM studies were critical for direct imaging of the conformational transitions of the cruciforms; however, the time scale of these observations does not relate to the characteristic times for transitions of cruciforms between the various conformations (*24*, *27*, *34*). In AFM, the majority of time the molecules remain bound to the surface, allowing for their reliable imaging by the scanning tip; therefore, the appearance of

the cruciform in a particular conformation is determined by how long the cruciform in this configuration stays at the surface. Therefore, time-lapse AFM studies provide the propensity of a molecule to adopt a particular conformation or shape rather than the lifetime of the conformation.

There are a number of interesting biological implications for the results obtained in this paper. The fact that supercoiling shifts the equilibrium between two conformations toward a folded conformation affects the dynamics of the juxtaposition of two sites in DNA required for such genetic processes as DNA site-specific recombination and transposition. The folded conformation of the cruciform restricts the slithering of the DNA domains relative to each other, whereas the unfolded one does not (*5*). There is a plethora of architectural and regulatory proteins that target DNA junctions, four-way junctions in particular (*10*, *12*, *14*, *35*). The finding that the geometry of the junctions is affected by DNA supercoiling suggests an additional mechanism for the involvement of DNA supercoiling into regulatory processes mediated by cruciforms. At the same time, within cells, DNA is supercoiled or arranged in topological domains; therefore, cruciforms are in fact natural models for Holliday junctions that are transient forms for DNA during recombination (homologous or site-specific) and aberrant pathways for DNA replication. Branch migration, either protein-mediated or spontaneous, is a critical step during these DNA transactions that require the unfolding of the junction (*19*, *27*, *30*, *31*). At the same time, the folding of the junction is needed for such processes as junction resolution (*14*). DNA topoisomerases are indispensable components of DNA replication and recombination machineries (*1*, *36*, *37*); therefore, controlling the Holliday junction geometry via changing the DNA supercoiling by topoisomerases is another potential regulatory pathway explaining the critical involvement of these enzymes in all DNA transactions.

ACKNOWLEDGMENT

We thank V. Potaman, Texas A&M University, for providing us with the topoisomer samples of plasmid DNA and M. Karymov and L. Shlyakhtenko for stimulating discussion of the data and critical comments and Alex Portillo for help in editing the manuscript.

SUPPORTING INFORMATION AVAILABLE

Descriptions of procedures for the preparation of the synthetic Holliday junction, measurements of interarm angle values and cruciform arm lengths, and movie files demonstrating dynamics of cruciform. This material is available free of charge via the Internet at http://pubs.acs.org.

REFERENCES

1. Sinden, R. R. (1994) *DNA Structure and Function*, Academic Press, San Diego, CA.
2. Kornberg, A., and Baker, T. A. (1992) *DNA Replication*, 2nd ed., Freeman, New York.
3. Jin, R., Fernandez-Beros, M. E., and Novick, R. P. (1997) Why is the initiation nick site of an AT-rich rolling circle plasmid at the tip of a GC-rich cruciform? *EMBO J. 16*, 4456−4466.
4. Dai, X., Greizerstein, M. B., Nadas-Chinni, K., and Rothman-Denes, L. B. (1997) Supercoil-induced extrusion of a regulatory DNA hairpin, *Proc. Natl. Acad. Sci. U.S.A. 94*, 2174−2179.
5. Shlyakhtenko, L. S., Hsieh, P., Grigoriev, M., Potaman, V. N., Sinden, R. R., and Lyubchenko, Y. L. (2000) A cruciform structural transition provides a molecular switch for chromosome structure and dynamics, *J. Mol. Biol. 296*, 1169−1173.
6. Lilley, D. M. (2000) Structures of helical junctions in nucleic acids, *Q. Rev. Biophys. 33*, 109−159.
7. Varga-Weisz, P., van Holde, K., and Zlatanova, J. (1993) Preferential binding of histone H1 to four-way helical junction DNA, *J. Biol. Chem. 268*, 20699−20700.
8. Varga-Weisz, P., Zlatanova, J., Leuba, S. H., Schroth, G. P., and van Holde, K. (1994) Binding of histones H1 and H5 and their globular domains to four-way junction DNA, *Proc. Natl. Acad. Sci. U.S.A. 91*, 3525−3529.
9. West, K. L., and Austin, C. A. (1999) Human DNA topoisomerase IIβ binds and cleaves four-way junction DNA in vitro, *Nucleic Acids Res. 27*, 984−992.
10. Pohler, J., Norman, D. G., Bramham, J., Bianchi, M. E., and Lilley, D. M. (1998) HMG box proteins bind to four-way DNA junctions in their open conformation, *EMBO J. 17*, 817−826.
11. Kamashev, D., and Rouviere-Yaniv, J. (2000) The histone-like protein HU binds specifically to DNA recombination and repair intermediates, *EMBO J. 19*, 6527−6535.
12. Lee, S., Cavallo, L., and Griffith, J. (1997) Human p53 binds Holliday junctions strongly and facilitates their cleavage, *J. Biol. Chem. 272*, 7532−7539.
13. Waldmann, T., Baack, M., Richter, N., and Gruss, C. (2003) Structure-specific binding of the proto-oncogene protein DEK to DNA, *Nucleic Acids Res. 31*, 7003−7010.
14. Khuu, P. A., Voth, A. R., Hays, F. A., and Ho, P. S. (2006) The stacked-X DNA Holliday junction and protein recognition, *J. Mol. Recognit. 19*, 234−242.
15. Zlatanova, J., and van Holde, K. (1998) Binding to four-way junction DNA: A common property of architectural proteins? *FASEB J. 12*, 421−431.
16. Hays, F. A., Watson, J., and Ho, P. S. (2003) Caution! DNA crossing: Crystal structures of Holliday junctions, *J. Biol. Chem. 278*, 49663−49666.
17. Clegg, R. M., Murchie, A. I., Zechel, A., Carlberg, C., Diekmann, S., and Lilley, D. M. (1992) Fluorescence resonance energy transfer analysis of the structure of the four-way DNA junction, *Biochemistry 31*, 4846−4856.
18. Joo, C., McKinney, S. A., Lilley, D. M., and Ha, T. (2004) Exploring rare conformational species and ionic effects in DNA Holliday junctions using single-molecule spectroscopy, *J. Mol. Biol. 341*, 739−751.
19. McKinney, S. A., Freeman, A. D., Lilley, D. M., and Ha, T. (2005) Observing spontaneous branch migration of Holliday junctions one step at a time, *Proc. Natl. Acad. Sci. U.S.A. 102*, 5715−5720.
20. Srinivasan, A. R., and Olson, W. K. (1994) Computer models of DNA four-way junctions, *Biochemistry 33*, 9389−9404.
21. Lu, M., Guo, Q., Seeman, N. C., and Kallenbach, N. R. (1991) Parallel and antiparallel Holliday junctions differ in structure and stability, *J. Mol. Biol. 221*, 1419−1432.
22. Oussatcheva, E. A., Pavlicek, J., Sankey, O. F., Sinden, R. R., Lyubchenko, Y. L., and Potaman, V. N. (2004) Influence of global DNA topology on cruciform formation in supercoiled DNA, *J. Mol. Biol. 338*, 735−743.
23. Pavlicek, J. W., Oussatcheva, E. A., Sinden, R. R., Potaman, V. N., Sankey, O. F., and Lyubchenko, Y. L. (2004) Supercoiling-induced DNA bending, *Biochemistry 43*, 10664−10668.
24. Shlyakhtenko, L. S., Potaman, V. N., Sinden, R. R., and Lyubchenko, Y. L. (1998) Structure and dynamics of supercoil-stabilized DNA cruciforms, *J. Mol. Biol. 280*, 61−72.
25. Lushnikov, A. Y., Brown, B. A., II, Oussatcheva, E. A., Potaman, V. N., Sinden, R. R., and Lyubchenko, Y. L. (2004) Interaction of the Zα domain of human ADAR1 with a negatively supercoiled plasmid visualized by atomic force microscopy, *Nucleic Acids Res. 32*, 4704−4712.
26. Shlyakhtenko, L. S., Gall, A. A., Filonov, A., Cerovac, Z., Lushnikov, A., and Lyubchenko, Y. L. (2003) Silatrane-based surface chemistry for immobilization of DNA, protein−DNA complexes and other biological materials, *Ultramicroscopy 97*, 279−287.
27. Lushnikov, A. Y., Bogdanov, A., and Lyubchenko, Y. L. (2003) DNA recombination: Holliday junctions dynamics and branch migration, *J. Biol. Chem. 278*, 43130−43134.
28. Lushnikov, A. Y., Potaman, V. N., Oussatcheva, E. A., Sinden, R. R., and Lyubchenko, Y. L. (2006) DNA strand arrangement within the *Sfi*I−DNA complex: Atomic force microscopy analysis, *Biochemistry 45*, 152−158.

29. Nollmann, M., Stark, W. M., and Byron, O. (2004) Low-resolution reconstruction of a synthetic DNA holliday junction, *Biophys. J. 86*, 3060−3069.
30. Panyutin, I. G., and Hsieh, P. (1994) The kinetics of spontaneous DNA branch migration, *Proc. Natl. Acad. Sci. U.S.A. 91*, 2021−2025.
31. Karymov, M., Daniel, D., Sankey, O. F., and Lyubchenko, Y. L. (2005) Holliday junction dynamics and branch migration: Single-molecule analysis, *Proc. Natl. Acad. Sci. U.S.A. 102*, 8186−8191.
32. Vologodskii, A. (1999) *Online Biophysical Chemistry Textbook*, Biophysical Society, Bethesda, MD.
33. Hohng, S., Joo, C., and Ha, T. (2004) Single-molecule three-color FRET, *Biophys. J. 87*, 1328−1337.
34. Lyubchenko, Y. L., and Shlyakhtenko, L. S. (1997) Visualization of supercoiled DNA with atomic force microscopy in situ, *Proc. Natl. Acad. Sci. U.S.A. 94*, 496−501.
35. Parsons, C. A., Stasiak, A., Bennett, R. J., and West, S. C. (1995) Structure of a multisubunit complex that promotes DNA branch migration, *Nature 374*, 375−378.
36. Hatfield, G. W., and Benham, C. J. (2002) DNA topology-mediated control of global gene expression in *Escherichia coli*, *Annu. Rev. Genet. 36*, 175−203.
37. Champoux, J. J. (2001) DNA topoisomerases: Structure, function, and mechanism, *Annu. Rev. Biochem. 70*, 369−413.

BI061002K